Article

THE STABILITY AND DISPERSION OF CARBON NANOTUBE-POLYMER SOLUTIONS: A MOLECULAR DYNAMICS STUDY

Sassan Jahangiri, Elif Ozden-Yenigun*

Abstract

Carbon nanotubes (CNTs) have been explored to increase the mechanical properties and electrical conductivity of polymeric fibers through compounding with polymer to be extruded into fibers. However, this route creates major challenges because CNTs have strong cohesion and tend to aggregate and precipitate due to their poor interfacial interaction with polymers. CNTs can be individualized from agglomerations to enhance the mechanical and electrical properties of polymer fibers but even so the capillary forces during solvent drying creates CNTs bundling. In this study, classical molecular dynamics (MD) simulations are used to predict and characterize CNTs-polymer interface mechanism in two different polymer matrices: polyvinyl butyral (PVB) and polystyrene-co-glycidyl methacrylate (P(St-*co*-GMA)). The dominated interface mechanisms are discovered to shed light on CNTs dispersion in solvent based systems and to explore the prerequisites for stabilized nanofluids. Our results showed that π-stacking interactions between aromatic groups and graphene surfaces of CNTs as in P(St-*co*-GMA) systems, play an important role in dispersion of CNTs, whereas slight repulsions between CNTs and PVB chains lead to large morphological differences and CNTs bundles in many chain systems. Altogether, the results indicated that polymers with structures having strong interactions with the surfaces of SWNTs through π-π interactions are more effective in dispersing CNTs and caused stabilized solutions in wet fiber processing.

Keywords

Molecular dynamics, nanofluids, carbon nanotubes, dispersion, composite fibers

Department of Textile Engineering, Istanbul Technical University, Turkey

Corresponding Author:

Elif Ozden-Yenigun, Department of Textile Engineering, Istanbul Technical University, Istanbul, 34437, Turkey

ITU Aerospace Research Center, Istanbul Technical University, Istanbul, 34469, Turkey

Email: ozdenyenigun@itu.edu.tr

Introduction

CNTs first reported by Oberlin *et al.* [1] and Iijima [2] have attracted attention of many scientists due to their unique mechanical, electrical and thermal properties. This form of carbon containing hexagons with concentric arrangement of cylinders has three distinctive types such as single-walled nanotubes (SWNTs), double-walled nanotubes (DWNTs) and multi-walled nanotubes (MWNTs). SWNTs have one tubular rolled layer of hexagonal carbon atoms with diameters ranging from 0.4 to 3 nm (Figure 1(a)) whereas MWNTs have several coaxial cylindrical layers with diameters up to 100 nm [3]. CNTs are excellent nano-reinforcement materials due to their low mass density, large aspect ratio and high elastic modulus (approximately 1 TPa [4]) and thus used in numerous applications such as composites [5-8], electrochemical devices [9-12], hydrogen storage [13-16], field emission devices [17-19], nanometer-sized electronic devices [20-22], sensors and probes [23-26] and fibers [27-29] etc. However, the superior performance of CNTs which depends on the distribution of length and diameter, the chirality, and its defect and impurities cannot as yet be fully transferred into macro-scale composites. Many studies investigated an appropriate scheme for transferring individual nanotubes properties into polymer composites [8, 9, 30-34]. In wet fiber processing, the major drawback is to obtain a good dispersion of CNTs by maintaining attractive interaction with the surrounding polymer matrix [8]. Moreover, it is also essential to stabilize this dispersion to prevent reaggregation of the CNTs throughout the processes.

In literature, several polymer matrices are reported for CNTs reinforced with nanofiber/fibers that benefit from CNTs-polymer attractive interactions [35-37]. For instance, recent experimental observations indicated that P(St-*co*-GMA) containing aromatic rings have attractive π-π interaction with the graphitic side walls of CNTs [38],which is called "π -stacking". This interaction leads to CNTs bundles which are major obstacles to their processing [39]. There are several techniques reported to overcome this challenge, particularly in wet fiber processing [40-43]. Homogenously dispersed polymer/nanotube solutions lead to well oriented CNTs in the resultant nanofibers/fibers. For instance, adding surfactants (e.g. sodium dodecyl sulphate), large amphiphilic polymers (e.g. polyvinyl pyrrolidone) and natural macromolecules (e.g. polysaccharide, Gum arabic) which can be adsorbed onto the hydrophobic nanotubes help to stabilize CNTs dispersions [44, 45]. In addition, ultrasonication is another useful technique to overcome the entanglement of nanotubes and to break up the agglomerates. However, it might cause some defects and irregularities into the CNTs [46]. Chemical functionalization of CNTs also helps to disperse CNTs, but it dominantly affects their electronic and photonic properties [47]. Different types of polymers, including polystyrene, polyurethane, polystyrene-co-glycidyl methacrylate (P(St-*co*-GMA)), poly (vinyl butyral) (PVB) have been used as polymer matrices to produce CNTs composite nanofibers [47-50]. Polymers containing aromatic rings are able to wrap CNTs via π-π stacking and van der Waals interactions between the polymer chain and nanotube surface [51]. Ozden-Yenigun *et al.* used surface reactive copolymer (P(St-*co*-GMA)) and successfully produced CNTs reinforced electrospun nanofibers without any modification, they reported the enhancement in flexural strength (15%) and flexural modulus (20%)

within the incorporation of CNTs into epoxy resin[38]. Charitidis *et al.* used PVB as matrix in CNTs integrated nanocomposites to enhance electrical and thermal properties [52, 53]. Later, Imaizumi *et al*. produced MWNTs/PVB composite electrospun nanofibers and twisted these nanofibers to have composite nanofiber yarns [54]. Enhanced mechanical, electrical and thermal properties were reported and explained by referring CNTs-PVB interactions. As seen in literature, P(St-co-GMA) (Figure 1(b)) and PVB (Figure 1(c)) are two different polymers that successfully promise CNTs oriented nanofibers. However, dominated mechanism in liquid state prior to fiber forming was not explained in detail. Herein we aimed to explore these two different polymer matrices' dispersing ability of CNTs, which are in different chemical nature.

Classical molecular dynamic (MD) simulations provide insight into interaction mechanism indifferent supramolecular systems [55, 56]. But still, computational cost of such simulations limits the construction of representative experimental models [56, 57]. MD simulation is frequently used to explore CNTs and their interactions in polymer matrices [58-63]. For instance, Uddin *et al.* investigated the effect of surfactant chemistry in CNTs/surfactant in water based solutions via MD [64]. They also reported the dominated dispersive interactions in CNTs/ Polyethylene oxide/water systems and pointed out the hydrophobic interactions of CNTs in water based solutions [65]. Pang *et al.* explored the dispersion state of CNTs in aqueous solutions and the wrapping motion of silicon surfactants experimentally and computationally and noted that van der Waals attractions leaded to steric stabilization [66]. Sohrabi *et al.* probed pure and mixed surfactants adsorption mechanism onto nanotubes via MD and revealed how surfactant approached to the surface and warp CNTs at low concentrations. [67]. In another study, Xiao *et al.* functionalized CNTs by covalent linking of alkyl chains and investigated these wrapping ability around CNTs, and discussed the aggregation behavior of functionalized CNTs via MD [68]. The results showed that CNTs without alkyl chains experienced smooth pullout, while those with alkyl chains underwent an uneven pullout by exhibiting five failure stages. In addition, the crystallization of polyethylene molecules occurred in the vicinity of CNTs which increased the interfacial shear strength by 15% [68].

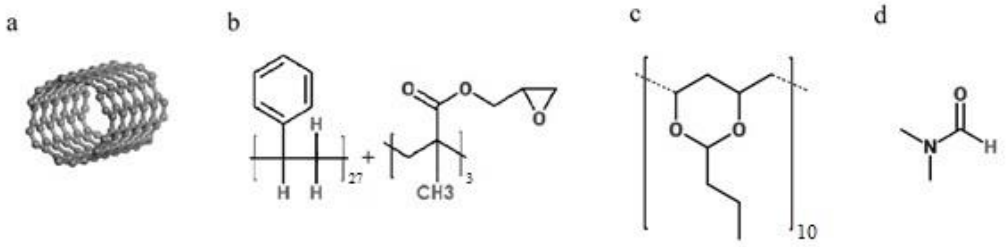

Figure 1. Molecular structures of (a): Ball and stick model of (6,6) single-walled CNTs with diameter of 8.14Å and length of 14.76Å sketched by Materials Studio ® 8.0 [69] and chemical structures of (b): Polystyrene-co-glycidyl methacrylate (P(ST-*co*-GMA)) (c): Poly(vinyl butyral) (PVB) (d): dimethylformamide (DMF).

In this study, MD simulations are used to predict and characterize polymer-CNTs interface mechanisms in PVB and P(St-*co*-GMA) polymer solutions which are proven

good polymer matrices for composite fibers without any further functionalization. [38, 70]. Thus, P(St-*co*-GMA) and PVB polymers are introduced into atomistic models to investigate and compare their interactions with CNTs by monitoring the effect of aromatic groups on CNTs dispersion. We also incorporate solvent molecules dimethylformamide (DMF) (Figure 1 (d)) to simulate solvent-based fiber solutions, as in wet-fiber processing. Local structure is evaluated by analyzing radial distribution function of CNTs concentration profile and radius of gyration of polymer to understand dominated particle-polymer interaction mechanism [71, 72]. Clustering behavior and single polymer dynamics of neat and CNTs containing polymer solutions are determined to provide insight into the nanofluids behavior at the macro-scale.

Materials and Methods

The molecular simulation software package Materials Studio® 8.0 [69] was used to construct the initial molecular structures, simulations and post-processing of the collected trajectories. COMPASS (Condensed-phase Optimized Molecular Potentials for Atomistic Simulation Studies) force field which was used in this study, has proven to be effective in defining properties of synthetic polymers [73]. Simulation boxes were constructed by Amorphous Cell module at target density of 1.0 g/cm^3 as in Table 1 and the number of molecules in both systems were adjusted to keep the number of atoms constant. Figure 2(a) and Figure 2(b) represent simulation boxes of PSTcoGMA-1-CNTs and PVB-1-CNTs, respectively. PVB polymer has 10 monomers while P(St-*co*-GMA) copolymer has 27 styrene monomers and 3 glycidyl methacrylate monomers. SWNTs were (6,6) single-walled CNTs with diameter of 8.14Å and length of 14.76Å (Figure 1(a)).MD simulations of the solvated systems were carried out in the isothermal-isobaric (NPT) statistical ensemble, at P=1 atm and T=300 K. To maintain temperature and pressure fixed at their prescribed values, the Andersen – thermostat [74] and Berendsen [75] barostat were used.

Table 1. Simulated models of PVB and P(St-co-GMA), construction parameters and their cell parameters for MD simulations.

P(St-co-GMA) Systems

Model Name	**# of polymer molecules**	**# of DMF Molecules**	**# of SWNTs**	**Cell Parameters (Å)**
PSTcoGMA-0-CNTs	5	50	0	32.03
PSTcoGMA-1-CNTs	5	50	1	39.05
PSTcoGMA-2-CNTs	5	50	2	40.07
PSTcoGMA-3-CNTs	5	50	3	41.04
PSTcoGMA-4-CNTs	5	50	4	41.96
PSTcoGMA-5-CNTs	5	50	5	42.84

PVB Systems

Model Name	**# of polymer molecules**	**# of DMF Molecules**	**# of SWNTs**	**Cell Parameters (Å)**
PVB-0-CNTs	10	100	0	32.95
PVB-1-CNTs	10	100	1	33.81
PVB-2-CNTs	10	100	2	41.05
PVB-3-CNTs	10	100	3	41.98
PVB-4-CNTs	10	100	4	42.87
PVB-5-CNTs	10	100	5	43.72

Each system was subject to detailed molecular dynamics simulations up to 20 ns. The trajectories of equilibrated systems were saved and analyzed by Materials Studio® Forcite Analysis Module to monitor structural changes. Local structure evolution was completed by analyzing structural parameters such as radial distribution functions (RDFs), CNTs concentration profile and radius of gyration (R_G) of polymers of the equilibrated trajectories. Pair correlation functions of each system including intra and intermolecular components were calculated at cutoff 12.5Å. Last 5ns trajectories were averaged out to determine concentration profiles of CNTs-CNTs pairs and RDFs of CNTs-CNTs, CNTs-DMF, and CNTs- PVB/P(St-*co*-GMA) pairs at different CNT concentrations, and to understand dominated clustering and dispersion properties, whereas R_G of PVB and P(St-*co*-GMA) molecules were explored to reveal single chain dynamics in presence of CNTs.

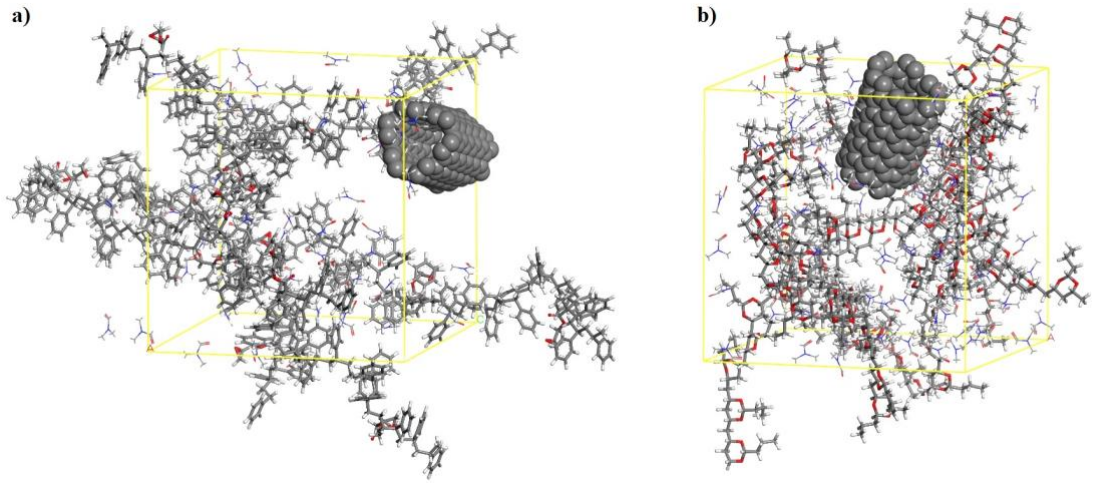

Figure 2. Constructed simulation boxes of (a): PSTcoGMA-1-CNTs and (b): PVB-1-CNTs systems which are described in Table 1. For better description, CNTs were displayed in CPK representation, while stick and line representations are preferred for polymer and solvent molecules, respectively.

Results and Discussion

Dispersion of CNTs in PVB/DMF systems

Molecular interactions between SWNTs, polymer and DMF solvent molecules were studied at different CNTs number densities as given in Table 1, to provide detailed information at the molecular level as well as to understand the dominated mechanism. First RDFs of PVB systems were calculated and RDFs of CNTs-CNTs, PVB-CNTs, and DMF-CNTs are displayed in Figures 3, respectively. Figure 3(a) and Figure 3(b) describe RDFs of CNTs-CNTs and PVB-CNTs at different CNTs number densities, which are complementary to describe short and long range of order in presence of CNTs in PVB/DMF solutions. Figure 3(a) revealed that the first coordination shell of CNTs–CNTs interactions ends at *ca.* 5 Å, displaying sharper distributions in PVB-2-CNTs and PVB-3-CNTs. RDFs of CNTs-PVB at around 5Å revealed that increasing CNTs concentration also altered polymer-CNTs interaction in short distances due to increase in probability of finding each other. While, at longer distances, as beyond 10Å, CNTs-CNTs interactions and CNT-PVB interaction were balanced. But still, because of the tendency of CNTs to prefer CNTs over polymer molecules, there will be an uneven distribution of CNTs and polymer molecules elsewhere. This could lead to CNTs clustering particularly in CNTs rich suspensions, which also pointed one of the major drawbacks to use CNTs at high loading levels (above 10 wt%). PVB-2-CNTs and PVB-3-CNTs systems revealed that although CNTs tend to agglomerate in low concentrations due to the "π-stacking" phenomena [76], in higher concentration models as in PVB-4-CNTs and PVB-5-CNTs, CNTs have to occupy the space in every coordinates (Figure 3(a)). It could be related to the abundance of the CNTs in the same cell box dimensions. We should also note that

Imaizumi *et al.* [54] observed highly oriented and individual MWNTs along fiber axis, at 10 wt% MWNT concentration, which was due to the electrified liquid flow formed during electrospinning. On the other hand, additive effect of the MWNT on the electrical conductivity of the as-spun composite fiber was quite limited. They concluded that the PVB matrix polymer blocked the electrical contacts between the nanotubes. We rationalize this outcome by considering the distribution of CNTs. In PVB systems, CNTs tend to cluster more with its own kind than the other species, which leads to prevent to build required network for electrical conductivity.

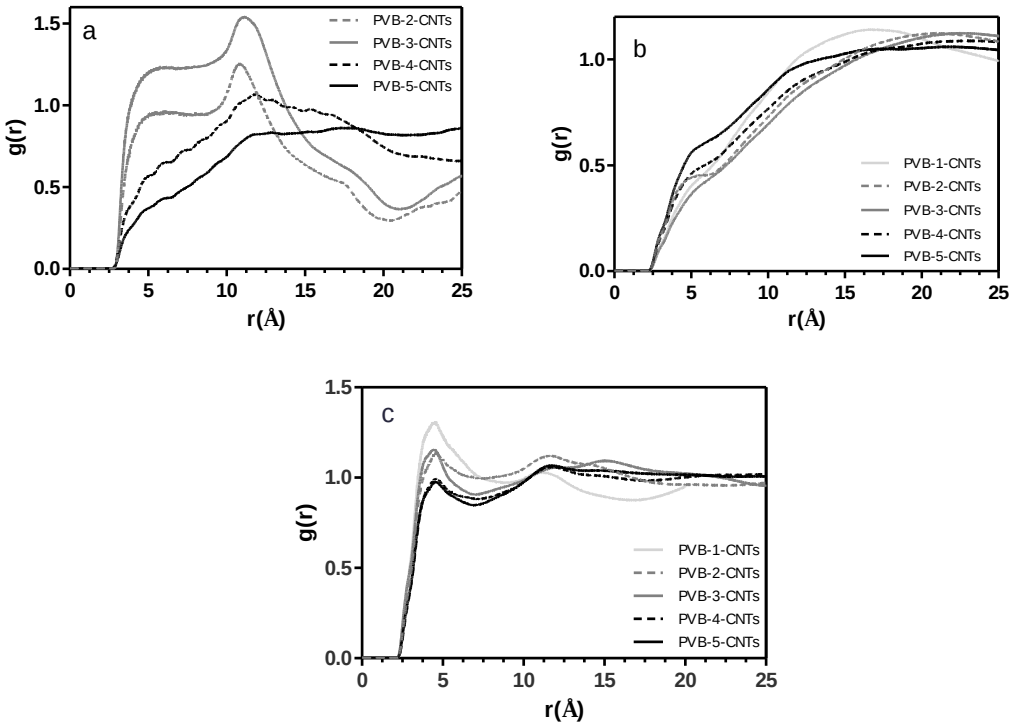

Figure 3. (a) Radial Distribution Function (RDF) of **CNTs-CNTs** in PVB-2-CNTs, PVB-3-CNTs, PVB-4-CNTs, PVB-5-CNTs models, (b) RDF of **PVB-CNTs** in PVB-1-CNTs, PVB-2-CNTs, PVB-3-CNTs, PVB-4-CNTs, PVB-5-CNTs models and (c) RDF of **DMF-CNTs** in PVB-1-CNTs, PVB-2-CNTs, PVB-3-CNTs, PVB-4-CNTs, PVB-5-CNTs models.

Even though, DMF solvent molecules are mobile enough, the tendency of DMF molecules towards CNTs are reduced by increased CNTs concentrations, as seen in Figure 3(c). Therefore, we observed that solvent choice does not provide additive effect to disperse CNTs in PVB systems. Single chain dynamics and dimensional stability could provide insight into attractive and repulsive interactions around polymer chains. The analysis on R_G expressed polymer chain conformations and exhibited how the gyration

radius changed due to these repulsive/attractive interactions. As seen in Figure 4, R_G of PVB chains were calculated at different CNTs concentrations. For better description, Gaussian fits of curves given in Figure 4 while raw data are also provided in Figure S1.

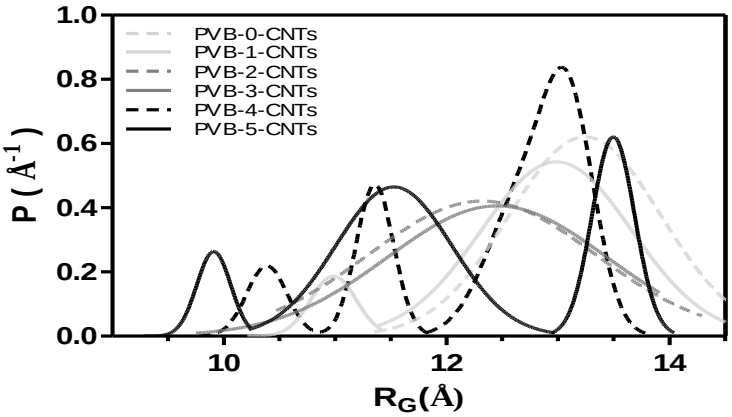

Figure 4. Gaussian fits of Radius of Gyration **(R_G)** of PVB molecules in all equilibrated PVB models.

The measures on chain size, R_G, carry information on the local chain geometry, which depends on valence and dihedral angle distributions as well as local interactions [77]. Figure 4 describes that with an increase in CNTs number density, R_G of PVB molecules slightly reduces. Due to repulsive interactions between CNTs-PVB, polymer molecules suffer from chain contractions. Moreover, three distinctive peaks were observed at higher polymer concentrations (*e.g.* PVB-4-CNTs and PVB-5-CNTs), and this could lead to CNTs rich and polymer rich regions in the polymer solutions, caused by uneven distribution of molecules. The small variations observed in chain dimensions and slight repulsions between CNTs and PVB chains lead to large morphological differences in many chain systems and eventually phase separations. Thus, the tendency of CNTs to agglomerate in PVB/DMF systems were explored by CNTs concentration profile analysis. Last 5 ns chunks of total 20ns dynamics of each equilibrated systems were analyzed to obtain CNTs concentration profiles in (100), (010) and (001) *hkl* planes. Figure 5 illustrates the CNT concentration profiles of PVB models in these 3 different planes respectively. In high concentration models, due to the abundance of the CNT molecules in the same cell-box dimensions, CNTs are standing more close to each other. In PVB models, even in high CNT concentration models, phase separation of CNT groups occurs (PVB-5-CNTs model at *ca.* 13 Å in (001) plane). Thus, it is clear that PVB polymers are not effective enough to disperse CNTs individually at atomistic level, they may require additional dispersing agents such as surfactants and/or dispersing method in wet fiber processing or electrohydrodynamic spinning process such as electrospinning.

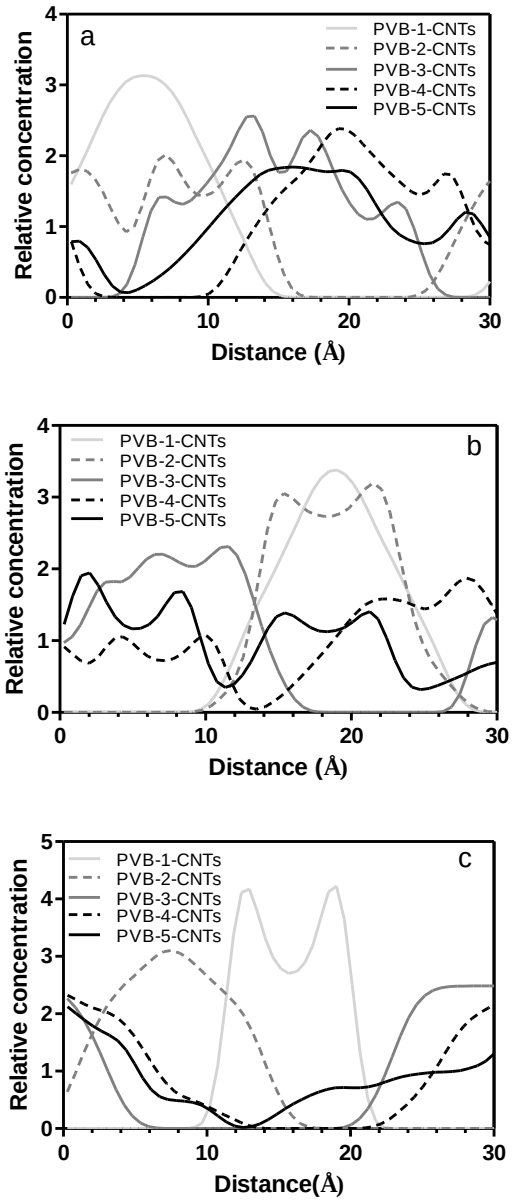

Figure 5. CNTs Concentration profile of PVB models with different CNT concentrations in given planes. (a) (100), (b) (010) and (c) (001)

Dispersion of CNTs in P(St-*co*-GMA)/DMF systems

The experimental observations pointed out that long-term stability of CNTs could be achieved by the manipulation of π-π interactions in P(St-*co*-GMA)/DMF systems [18]. Thus as seen in Figure 6, P(St-*co*-GMA) models demonstrate different interaction mechanisms than PVB models. Figure 6(a) and Figure 6(b) exhibit RDF of CNTs-CNTs and CNTs-P(St-co-GMA) at different CNTs concentrations, respectively. As seen in Figure 6(a),

there was no long range order for CNTs. A peak at around 12.5 Å was observed which would be due to neighboring walls of CNTs considering the diameter of individual CNTs which is approximately 8.14 Å. The tendency of the CNTs clustering together is not as strong as it is in PVB systems. Figure 6(b) addressed that polymer has affinity towards CNTs both in short range and long range distances. This difference might be based on the presence of aromatic groups in P(St-*co*-GMA), that provide strong short-range interactions with nanotube sidewalls. It can be also seen from Figure 6(b) that due to aromatic ring groups, P(St-*co*-GMA) molecules were positioned closer to CNTs sidewalls than PVB molecules. This further supports our prediction that there could be strong alignment of aromatic rings of P(St-*co*-GMA) parallel to the carbon nanotube surface [43, 78]. As has been recently demonstrated with aromatic amino acids [78], the stacking of aromatic groups onto the SWNT surface allows for the dispersion of individual SWNTs. Moreover, the incorporation of aromatic groups decreases the ability of the peptides to self-associate, which was also revealed in atomic force microscope images. Intensive π-π interaction between these polycyclic aromatic hydrocarbons and the external SWCNT surface were demonstrated by experimental findings [79, 80]. As in P(St-*co*-GMA) molecules, rigid-backbone polymers are able to form ordered molecular structures surrounding the nanotubes with n-fold symmetry, expressed by Nish *et.al [81]*. At longer distances beyond 12.5 Å, P(St-*co*-GMA) molecules still maintain their tendency towards CNTs as seen in Figure 6(b). This can be interpreted as the dispersing ability of styrene based polymers, which could be an effective agent in wet-fiber processing. Thus, it is predictable that isolation of individual CNTs could be achieved with a polymer design containing aromatic groups. RDFs of DMF-CNTs (Figure 6(c)), in presence of P(St-co-GMA) displays almost same profile as in PVB models and at longer distances, DMF-CNTs interactions are diminished while increasing CNTs concentrations whereas styrene based polymers are more soluble in DMF than PVB. The selective dispersion have been found to be strongly influenced by the polymer structures and solvent used [82].

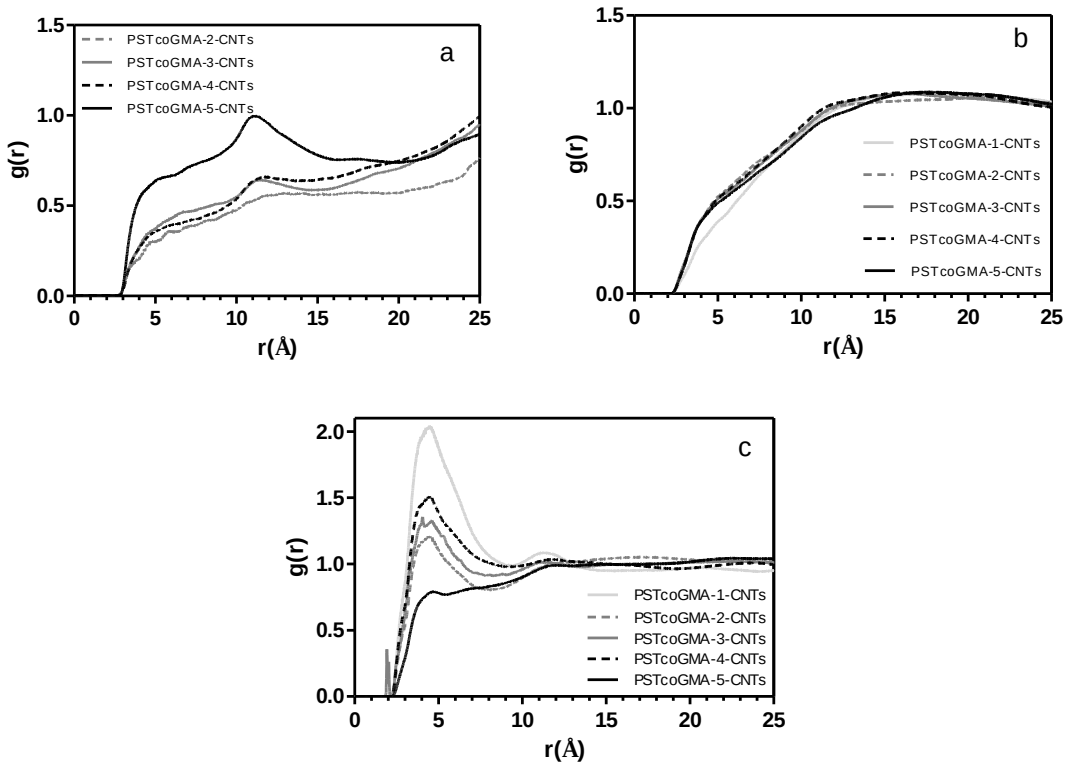

Figure 6. (a) RDF of **CNTs-CNTs** in PSTcoGMA-2-CNTs, PSTcoGMA-3-CNTs and PSTcoGMA-4-CNTs and PSTcoGMA-5-CNTs models (b) RDF of **CNTs-P(St-*co*-GMA)** in PSTcoGMA-1-CNTs, PSTcoGMA-2-CNTs, PSTcoGMA-3-CNTs, PSTcoGMA-4-CNTs and PSTcoGMA-5-CNTs models (c) RDF of **DMF-CNTs** in PSTcoGMA-1-CNTs, PSTcoGMA-2-CNTs, PSTcoGMA-3-CNTs, PSTcoGMA-4-CNTs and PSTcoGMA-5-CNTs models.

Figure 7 displays R_G of P(St-*co*-GMA) molecules at different CNT number densities. For better description, Gaussian fits of curves are given in Figure 7 while raw data are also provided in Figure S2. The mean peak value of R_G for the P(St-*co*-GMA) molecule in absence of CNTs (*e.g.* PSTcoGMA-0-CNTs) was about 20Å whereas in PSTcoGMA-5-CNTs model two distinctive peaks were observed, the mean value was shifted to 15.6Å. We observed that with an increase in CNTs concentration, R_G of P(St-*co*-GMA) molecules slightly decreases, as in PVB models. Furthermore, the shift of R_G in presence of CNTs was below 5 Å (from 20.0 to 15.6 Å) whereas the end to end distance of P(St-*co*-GMA) was approximately 70 Å. In case of PVB, this dimensional change was about 3 Å where the end to end distance of PVBs was around 50 Å. Therefore, we can conclude that PVB molecules have almost the same contraction value (%) as P(St-*co*-GMA) molecules. However, in case of P(St-*co*-GMA) systems, polymer molecules suffer more due to the π-π interactions between the aromatic rings of P(St-*co*-GMA) on their chains and not between the aromatic rings of P(St-*co*-GMA) and CNTs. Concentration profile of CNTs given in Figure 8 would also assist to understand these same-kind interactions. Unlike PVB models, P(St-*co*-GMA) models exhibited better dispersion state in high

CNTs loadings. Thus, no phase separation was observed in PSTcoGMA-4-CNTs and PSTcoGMA-5-CNTs models (Figure 8). This is further evidence of how that better dispersion of CNTs in the vicinity of P(St-*co*-GMA) molecules was achieved due to the increased π-π stacking with a strong orientation preference.

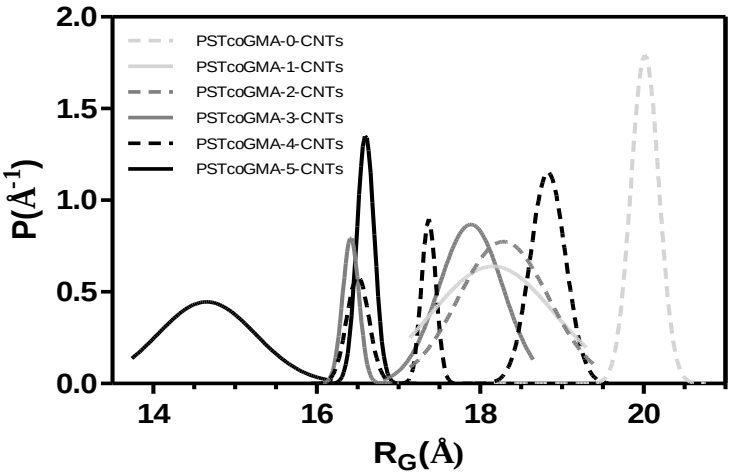

Figure 7. Gaussian fits of $\mathbf{R_G}$ of P(St-*co*-GMA) molecules in all equilibrated PSTcoGMA models.

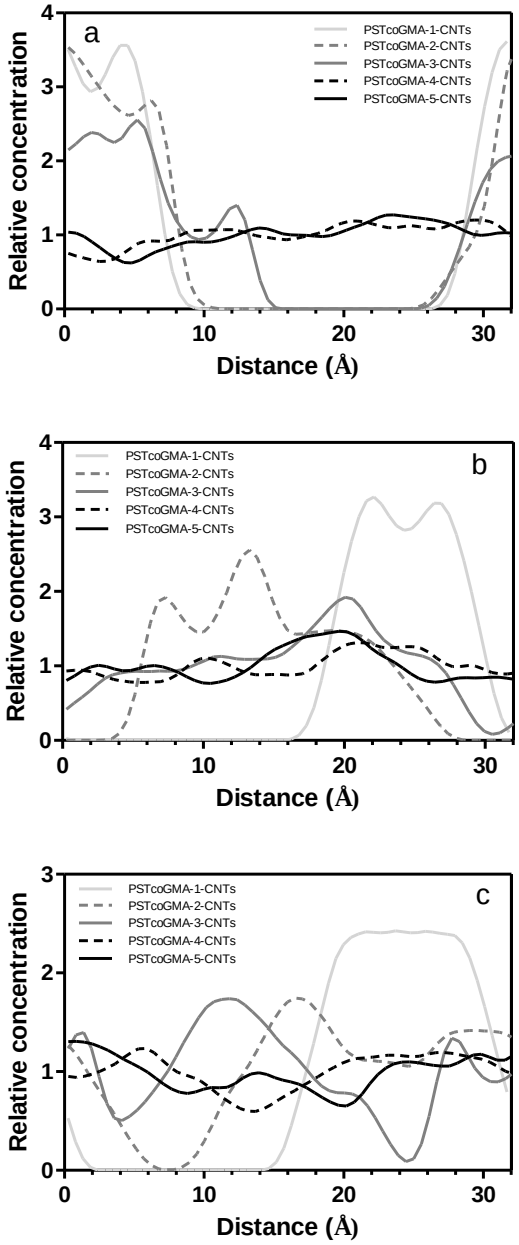

Figure 8. CNTs Concentration profile of P(St-*co*-GMA) models with different CNT concentrations in given planes. (a) (100), (b) (010) and (c) (001).

Conclusion

In conclusion, local structures and conformational analysis in presence of CNTs are performed to provide insight into dispersing ability of PVB and P(St-*co*-GMA) molecules. It is seen that due to the π-π interactions between the aromatic rings of P(St-*co*-GMA) and CNTs, P(St-*co*-GMA) molecules were more effective in dispersing CNTs and/or preventing CNTs clusters than PVB molecules. PVB-CNTs interactions influence the

degree of dispersion of the nanotubes and polymer reaggregation. Additional dispersing agents such as surfactants in wet fiber processing or electrohydrodynamic spinning process were required to form composite PVB fibers. We can conclude that polymers, which contain aromatic rings, are better candidates to disperse CNTs in wet fiber processing. Manipulating the π-π interactions between these aromatic rings and CNTs, would eliminate the need of dispersing agents in fiber forming.

ACKNOWLEDGEMENT

This study is funded by **TUBITAK** (Grant Number: **213M618**), under R&D Projects funding program.

References

1. Oberlin A, Endo M and Koyama T. Filamentous Growth of Carbon through Benzene Decomposition. *J Cryst Growth* 1976; 32: 335-349.
2. Iijima S. Helical Microtubules of Graphitic Carbon. *Nature* 1991; 354: 56-58.
3. Baughman RH, Zakhidov AA and de Heer WA. Carbon nanotubes - the route toward applications. *Science* 2002; 297: 787-792.
4. Lu JP. Elastic properties of single and multilayered nanotubes. *J Phys Chem Solids* 1997; 58: 1649-1652.
5. Mansoor M and Shahid M. Carbon nanotube-reinforced aluminum composite produced by induction melting. *J Appl Res Technol* 2016; 14: 215-224.
6. Peng C, Zhang S, Jewell D, et al. Carbon nanotube and conducting polymer composites for supercapacitors. *Prog Nat Sci* 2008; 18: 777-788.
7. Sivakkumar SR, Howlett PC, Winther-Jensen B, et al. Polyterthiophene/CNT composite as a cathode material for lithium batteries employing an ionic liquid electrolyte. *Electrochim Acta* 2009; 54: 6844-6849.
8. Spitalsky Z, Tasis D, Papagelis K, et al. Carbon nanotube-polymer composites: Chemistry, processing, mechanical and electrical properties. *Prog Polym Sci* 2010; 35: 357-401.
9. Bauhofer W and Kovacs JZ. A review and analysis of electrical percolation in carbon nanotube polymer composites. *Compos Sci Technol* 2009; 69: 1486-1498.
10. Herrasti Z, Martínez F and Baldrich E. CNT Wiring for Signal Amplification in Electrochemical Magnetosensors. *Procedia Eng* 2014; 87: 712-715.
11. Jacobs CB, Peairs MJ and Venton BJ. Review: Carbon nanotube based electrochemical sensors for biomolecules. *Anal Chim Acta* 2010; 662: 105-127.
12. Musameh M, Lawrence NS and Wang J. Electrochemical activation of carbon nanotubes. *Electrochem Commun* 2005; 7: 14-18.
13. Chen YL, Liu B, Wu J, et al. Mechanics of hydrogen storage in carbon nanotubes. *J Mech Phys Solids* 2008; 56: 3224-3241.

14. Cheng H-M, Yang Q-H and Liu C. Hydrogen storage in carbon nanotubes. *Carbon* 2001; 39: 1447-1454.
15. Darkrim FL, Malbrunot P and Tartaglia GP. Review of hydrogen storage by adsorption in carbon nanotubes. *Int J Hydrogen Energ* 2002; 27: 193-202.
16. Tibbetts GG, Meisner GP and Olk CH. Hydrogen storage capacity of carbon nanotubes, filaments, and vapor-grown fibers. *Carbon* 2001; 39: 2291-2301.
17. Jang HS, Lee H-R and Kim D-H. Field emission properties of carbon nanotubes with different morphologies. *Thin Solid Films* 2006; 500: 124-128.
18. Lee NS, Chung DS, Han IT, et al. Application of carbon nanotubes to field emission displays. *Diamond Relat Mater* 2001; 10: 265-270.
19. Saito Y and Uemura S. Field emission from carbon nanotubes and its application to electron sources. *Carbon* 2000; 38: 169-182.
20. Biswas C and Lee YH. Graphene Versus Carbon Nanotubes in Electronic Devices. *Adv Funct Mater* 2011; 21: 3806-3826.
21. Léonard F. Chapter 4 - Electronic Devices. *The Physics of Carbon Nanotube Devices*. Norwich, NY: William Andrew Publishing, 2009, pp.75-136.
22. Peng L-M, Zhang Z and Wang S. Carbon nanotube electronics: recent advances. *Mater Today* 2014; 17: 433-442.
23. Chowdhury R, Adhikari S and Mitchell J. Vibrating carbon nanotube based bio-sensors. *Physica E Low Dimens Syst Nanostruct* 2009; 42: 104-109.
24. Hirotani J, Amano J, Ikuta T, et al. Carbon nanotube thermal probe for quantitative temperature sensing. *Sens Actuators A Phys* 2013; 199: 1-8.
25. Li C and Shi G. Carbon nanotube-based fluorescence sensors. *J Photochem Photobiol C: Photochem Rev* 2014; 19: 20-34.
26. Ménard-Moyon C, Kostarelos K, Prato M, et al. Functionalized Carbon Nanotubes for Probing and Modulating Molecular Functions. *Chem Biol* 2010; 17: 107-115.
27. Chen W, Tao X and Liu Y. Carbon nanotube-reinforced polyurethane composite fibers. *Compos Sci Technol* 2006; 66: 3029-3034.
28. Deng F, Lu W, Zhao H, et al. The properties of dry-spun carbon nanotube fibers and their interfacial shear strength in an epoxy composite. *Carbon* 2011; 49: 1752-1757.
29. Wu AS and Chou T-W. Carbon nanotube fibers for advanced composites. *Mater Today* 2012; 15: 302-310.
30. Andrews R and Weisenberger MC. Carbon nanotube polymer composites. *Curr Opin Solid State Mater Sci* 2004; 8: 31-37.
31. Coleman JN, Khan U, Blau WJ, et al. Small but strong: A review of the mechanical properties of carbon nanotube–polymer composites. *Carbon* 2006; 44: 1624-1652.
32. Camponeschi E, Vance R, Al-Haik M, et al. Properties of carbon nanotube–polymer composites aligned in a magnetic field. *Carbon* 2007; 45: 2037-2046.
33. Ahir SV, Huang YY and Terentjev EM. Polymers with aligned carbon nanotubes: Active composite materials. *Polymer* 2008; 49: 3841-3854.
34. Gupta A and Choudhary V. Electrical conductivity and shielding effectiveness of poly(trimethylene terephthalate)/multiwalled carbon nanotube composites. *J Mater Sci* 2011; 46: 6416-6423.
35. Ye H, Lam H, Titchenal N, et al. Reinforcement and rupture behavior of carbon nanotubes–polymer nanofibers. *Appl Phys Lett* 2004; 85: 1775-1777.

36. Taguet A, Cassagnau P and Lopez-Cuesta JM. Structuration, selective dispersion and compatibilizing effect of (nano)fillers in polymer blends. *Prog Polym Sci* 2014; 39: 1526-1563.
37. Rahman MM, Hussein MA, Alamry KA, et al. Sensitive methanol sensor based on PMMA-G-CNTs nanocomposites deposited onto glassy carbon electrodes. *Talanta* 2016; 150: 71-80.
38. Ozden-Yenigun E, Menceloglu YZ and Papila M. MWCNTs/P(St-co-GMA) Composite Nanofibers of Engineered Interface Chemistry for Epoxy Matrix Nanocomposites. *Acs Appl Mater Inter* 2012; 4: 777-784.
39. Tan YQ and Resasco DE. Dispersion of single-walled carbon nanotubes of narrow diameter distribution. *J Phys Chem B* 2005; 109: 14454-14460.
40. Kearns JC and Shambaugh RL. Polypropylene fibers reinforced with carbon nanotubes. *J Appl Polym Sci* 2002; 86: 2079-2084.
41. Xie X-L, Mai Y-W and Zhou X-P. Dispersion and alignment of carbon nanotubes in polymer matrix: A review. *Mater Sci and Eng, R* 2005; 49: 89-112.
42. Leyton P, Gómez-Jeria JS, Sanchez-Cortes S, et al. Carbon Nanotube Bundles as Molecular Assemblies for the Detection of Polycyclic Aromatic Hydrocarbons: Surface-Enhanced Resonance Raman Spectroscopy and Theoretical Studies. *J Phys Chem B* 2006; 110: 6470-6474.
43. Meng L, Fu C and Lu Q. Advanced technology for functionalization of carbon nanotubes. *Prog Nat Sci* 2009; 19: 801-810.
44. Dror Y, Salalha W, Pyckhout-Hintzen W, et al. From carbon nanotube dispersion to composite nanofibers. *Scattering Methods and the Properties of Polymer Materials*. Springer Berlin Heidelberg, 2005, pp.64-69.
45. Dror Y, Salalha W, Khalfin RL, et al. Carbon nanotubes embedded in oriented polymer nanofibers by electrospinning. *Langmuir* 2003; 19: 7012-7020.
46. Naebe M, Lin T and Wang X. *Carbon nanotubes reinforced electrospun polymer nanofibres*. Rijeka, Croatia: InTech, 2010, p.309-328.
47. Mylvaganam K and Zhang LCC. Fabrication and Application of Polymer Composites Comprising Carbon Nanotubes. *Recent Pat Nanotech* 2007; 1: 59-65.
48. Sen R, Zhao B, Perea D, et al. Preparation of single-walled carbon nanotube reinforced polystyrene and polyurethane nanofibers and membranes by electrospinning. *Nano Lett* 2004; 4: 459-464.
49. Pan C, Ge L-Q and Gu Z-Z. Fabrication of multi-walled carbon nanotube reinforced polyelectrolyte hollow nanofibers by electrospinning. *Compos Sci Technol* 2007; 67: 3271-3277.
50. Kim GM, Michler GH and Pötschke P. Deformation processes of ultrahigh porous multiwalled carbon nanotubes/polycarbonate composite fibers prepared by electrospinning. *Polymer* 2005; 46: 7346-7351.
51. Vijay Kumar Thakur MKT. Chemical Functionalization of Carbon Nanomaterials: Chemistry and applications. *Chemical Functionalization of Carbon Nanomaterials*. CRC Press, 2015, pp.833.
52. Li Y, Yu T, Pui T, et al. Fabrication and characterization of recyclable carbon nanotube/polyvinyl butyral composite fiber. *Compos Sci Technol* 2011; 71: 1665-1670.

53. Charitidis CA, Koumoulos EP, Giorcelli M, et al. Nanomechanical and Tribological Properties of Carbon Nanotube/Polyvinyl Butyral Composites. *Polym Compos* 2013; 34: 1950-1960.
54. Imaizumi S, Matsumoto H, Konosu Y, et al. Top-Down Process Based on Electrospinning, Twisting, and Heating for Producing One-Dimensional Carbon Nanotube Assembly. *Acs Appl Mater Inter* 2011; 3: 469-475.
55. Fatemi SM and Foroutan M. Recent developments concerning the dispersion of carbon nanotubes in surfactant/polymer systems by MD simulation. *J Nanostructure Chem* 2016; 6: 29-40. journal article.
56. Calvaresi M, Hoefinger S and Zerbetto F. Probing the structure of lysozyme-carbon-nanotube hybrids with molecular dynamics. *Chemistry (Weinheim an der Bergstrasse, Germany)* 2012; 18: 4308-4313. 2012/02/23.
57. Pal G and Kumar S. Modeling of carbon nanotubes and carbon nanotube–polymer composites. *Prog Aerosp Sci* 2016; 80: 33-58.
58. Agrawal PM, Sudalayandi BS, Raff LM, et al. Molecular dynamics (MD) simulations of the dependence of C–C bond lengths and bond angles on the tensile strain in single-wall carbon nanotubes (SWCNT). *Comput Mater Sci* 2008; 41: 450-456.
59. Dilrukshi KGS, Dewapriya MAN and Puswewala UGA. Size dependency and potential field influence on deriving mechanical properties of carbon nanotubes using molecular dynamics. *Theor Appl Mech Lett* 2015; 5: 167-172.
60. Parsa MH, Zamani C, Babaei A, et al. Multi-scale Simulation of Carbon Nanotubes Interactions with Cell Membrane: DFT Calculations and Molecular Dynamic Simulation. *Procedia Mater Sci* 2015; 11: 423-427.
61. Rajesh R, Ganesh K, Lenny Koh SC, et al. Comparative Molecular Dynamics Simulation Study of Mechanical Properties of Carbon Nanotubes with Number of Stone-Wales and Vacancy Defects. *Procedia Eng* 2012; 38: 2347-2355.
62. Saha LCM, Shabeer A. ;Jang, Joon Kyung Molecular Dynamics Simulation Study on the Carbon Nanotube Interacting with a Polymer. *B Kor Chem Soc* 2012; 43: 893-896.
63. Wong CH and Vijayaraghavan V. Compressive characteristics of single walled carbon nanotube with water interactions investigated by using molecular dynamics simulation. *Phys Lett A* 2014; 378: 570-576.
64. Uddin NM, Capaldi FM and Farouk B. Molecular dynamics simulations of carbon nanotube dispersions in water: Effects of nanotube length, diameter, chirality and surfactant structures. *Comput Mater Sci* 2012; 53: 133-144.
65. Uddin NM, Capaldi FM and Farouk B. Molecular dynamics simulations of the interactions and dispersion of carbon nanotubes in polyethylene oxide/water systems. *Polymer* 2011; 52: 288-296.
66. Pang J, Xu G, Yuan S, et al. Dispersing carbon nanotubes in aqueous solutions by a silicon surfactant: Experimental and molecular dynamics simulation study. *Colloids Surf A: Physicochem Eng Asp* 2009; 350: 101-108.
67. Sohrabi B, Poorgholami-Bejarpasi N and Nayeri N. Dispersion of Carbon Nanotubes Using Mixed Surfactants: Experimental and Molecular Dynamics Simulation Studies. *J Phys Chem B* 2014; 118: 3094-3103.

68. Xiao T, Liu J and Xiong H. Effects of different functionalization schemes on the interfacial strength of carbon nanotube polyethylene composite. *Acta Mech Solida Sin* 2015; 28: 277-284.
69. Materials studio 8.0. *Materials Studio*. 8.0 ed. BIOVIA Corporate Americas, 5005 Wateridge Vista Drive, San Diego, CA, 92121, USA: Accelrys, 2015.
70. Peng T and Chang I. Uniformly dispersion of carbon nanotube in aluminum powders by wet shake-mixing approach. *Powder Technol* 2015; 284: 32-39.
71. Yang M, Koutsos V and Zaiser M. Interactions between polymers and carbon nanotubes: a molecular dynamics study. *J Phys Chem B* 2005; 109: 10009-10014. 2006/07/21.
72. Han Y and Elliott J. Molecular dynamics simulations of the elastic properties of polymer/carbon nanotube composites. *Comput Mater Sci* 2007; 39: 315-323.
73. Sun H. COMPASS: An ab initio force-field optimized for condensed-phase applications - Overview with details on alkane and benzene compounds. *J Phys Chem B* 1998; 102: 7338-7364.
74. Andersen HC. Molecular-Dynamics Simulations at Constant Pressure and-or Temperature. *J Chem Phys* 1980; 72: 2384-2393.
75. Berendsen HJC, Postma JPM, Vangunsteren WF, et al. Molecular-Dynamics with Coupling to an External Bath. *J Chem Phys* 1984; 81: 3684-3690.
76. Hélène C and Lancelot G. Interactions between functional groups in protein-nucleic acid associations. *Prog Biophys Mol Biol* 1982; 39: 1-68.
77. Ozden-Yenigun E, Simsek E, Menceloglu YZ, et al. Molecular basis for solvent dependent morphologies observed on electrosprayed surfaces. *Phys Chem Chem Phys* 2013; 15: 17862-17872. 10.1039/C3CP53079E.
78. Zorbas V, Smith AL, Xie H, et al. Importance of aromatic content for peptide/single-walled carbon nanotube interactions. *J Am Chem Soc* 2005; 127: 12323-12328. 2005/09/01.
79. Gotovac S, Honda H, Hattori Y, et al. Effect of nanoscale curvature of single-walled carbon nanotubes on adsorption of polycyclic aromatic hydrocarbons. *Nano Lett* 2007; 7: 583-587. 2007/02/24.
80. Zhao J, Lu JP, Han J, et al. Noncovalent functionalization of carbon nanotubes by aromatic organic molecules. *Appl Phys Lett* 2003; 82: 3746-3748.
81. Nish A, Hwang J-Y, Doig J, et al. Highly selective dispersion of single-walled carbon nanotubes using aromatic polymers. *Nat Nano* 2007; 2: 640-646. 10.1038/nnano.2007.290.
82. Hwang J-Y, Nish A, Doig J, et al. Polymer Structure and Solvent Effects on the Selective Dispersion of Single-Walled Carbon Nanotubes. *J Am Chem Soc* 2008; 130: 3543-3553.